How to cite: *Angew. Chem. Int. Ed.* **2023**, *62*, e202312147
doi.org/10.1002/anie.202312147

Hybrid Microbial Batteries

Super-fast Charging Biohybrid Batteries through a Power-to-formate-to-bioelectricity Process by Combining Microbial Electrochemistry and CO_2 Electrolysis

Na Chu, Yong Jiang, Donglin Wang, Daping Li, and Raymond Jianxiong Zeng*

Abstract: Extensive study on renewable energy storage has been sparked by the growing worries regarding global warming. In this study, incorporating the latest advancements in microbial electrochemistry and electrochemical CO_2 reduction, a super-fast charging biohybrid battery was introduced by using pure formic acid as an energy carrier. CO_2 electrolyser with a slim-catholyte layer and a solid electrolyte layer was built, which made it possible to use affordable anion exchange membranes and electrocatalysts that are readily accessible. The biohybrid battery only required a 3-minute charging to accomplish an astounding 25-hour discharging phase. In the power-to-formate-to-bioelectricity process, bioconversion played a vital role in restricting both the overall Faradaic efficiency and Energy efficiency. The CO_2 electrolyser was able to operate continuously for an impressive total duration of 164 hours under Gas Stand-By model, by storing N_2 gas in the extraction chamber during stand-by periods. Additionally, the electric signal generated during the discharging phase was utilized for monitoring water biotoxicity. Functional genes related to formate metabolism were identified in the bioanode and electrochemically active bacteria were discovered. On the other hand, *Paracoccus* was predominantly found in the used air cathode. These results advance our current knowledge of exploiting biohybrid technology.

[*] N. Chu, Prof. Y. Jiang, Prof. R. J. Zeng
Fujian Provincial Key Laboratory of Soil Environmental Health and Regulation, College of Resources and Environment
Fujian Agriculture and Forestry University
Fuzhou 350002 (China)
E-mail: jiangyongchange@163.com

N. Chu, Prof. Dr. D. Li
CAS Key Laboratory of Environmental and Applied Microbiology, Environmental Microbiology Key Laboratory of Sichuan Province, Chengdu Institute of Biology,
Chinese Academy of Sciences
Chengdu 610041 (China)

N. Chu
University of Chinese Academy of Sciences
Beijing 100049 (China)

Dr. D. Wang
Key Laboratory of Drinking Water Science and Technology, Research Center for Eco-Environmental Sciences,
Chinese Academy of Sciences
Beijing 100085 (China)

Introduction

In response to growing concerns about global warming, there has been a strong emphasis on the exploration of renewable energy sources. Thus, energy storage techniques and devices are becoming necessities, to match the variability in the generation of renewable energy with a fluctuating demand.[1] Formate is a remarkable energy carrier that truly stands out from the rest, to close the energy cycle. It is not only safer than hydrogen but also has the unique ability to store CO_2.[2] In addition, formate exhibits a high selectivity in its generation, surpassing other energy carriers with longer carbon chains, such as acetate.[3]

In the realm of energy storage, numerous techniques have demonstrated their ability to generate formate from CO_2. However, the application of chemical catalysis has faced certain limitations, including the reliance on noble metals and the need for extreme reaction conditions.[1,4] Therefore, significant efforts have been dedicated to the development of bioelectrocatalytic synthesis for low-cost formate production. Certain autotrophic bacteria, such as *Thermoanaerobacter kivui*, have demonstrated the ability to convert H_2 and CO_2 into formate. This process is catalyzed by hydrogen-dependent CO_2 reductase (HDCR), of which the structure has been revealed using cryo-electron microscopy recently.[5] Generally, the state-of-art bioelectrocatalytic synthesis process still faces the challenge of low conversion activity and low stability. For example, the current density of cathodic biofilm or enzymatic bioelectrocatalysis-based CO_2 fixation is generally found to be at least one order of magnitude lower than that of electrochemical CO_2 reduction (CO_2RR).[6] Strategies were required to block the ATP-dependent further microbial conversion of formate, by using ionophores, limiting the coupling ion, or inhibiting of the ATP synthase with engineering strains. In addition, only 30 % of the initial formate formation rate was presented, after 2 weeks of bioreactor operation when using *Acetobacterium woodii* as the biocatalyst.[2a] These limitations might restrict the using of bioelectrocatalytic synthesis as a standalone process for energy storage.

Recently, CO_2RR is receiving much attention as a promising energy storage technology, operated at low temperature and pressure.[7] To overcome the mass transport limitation, a gas diffusion electrode (GDE) is required in CO_2 electrolysers,[7b] thus enabled a super-fast energy storage process. Conventionally, after CO_2RR, the formate is dissolved in catholyte containing a significantly high

concentration of salt, such as KOH or $KHCO_3$.[8] Fortunately, a solid electrolyte can be adopted in CO_2 electrolysers to produce pure formic acid directly, which is regarded as one major advance in the past five years.[9] In the solid electrolyte layer, pure formic acid is in situ formed after the electrochemically generated $HCOO^-$ and H^+ crossed the membranes, respectively.[10] The direct production of pure formic acid not only eliminates the expenses associated with subsequent purification processes when using CO_2RR as a standalone technology but also paves the way for innovative biohybrid technologies by addressing the issue of apoptosis caused by the high concentration of salt.[11]

For energy recovery, as an energy carrier, formate generated from CO_2RR can be used as the starting reagent for direct formate fuel cells.[12] Furthermore, formate can be served as the substrate of microbes and enzymes. For example, the reversible interconversion of CO_2 into formate was demonstrated in semiartificial systems, consisting of formate dehydrogenase (FDH) and hydrogenase (H_2ase) from *Desulfovibrio vulgaris*.[13] Most importantly, formate can be used by electrochemically active bacteria (EAB), e.g., *Geobacter sulfurreducens*, for bioelectricity generation.[14] When microbial electrochemical reactors are used for energy recovery, a long-duration discharging phase is expected due to a much lower bioconversion activity. In fact, microbial electrochemical reactors can actually fulfill specific niche applications that cannot be achieved by other technologies, such as direct formate fuel cells. For instance, microbial electrochemical sensors can be used to monitor water biotoxicity by tracking the electric signals, identifying the bioavailable concentration of toxicants, and analyzing the resulting biological response to these substances.[15]

In this study, a novel biohybrid battery was created to close the energy cycle, inspired by cutting-edge advancements in microbial electrochemistry and CO_2 electrolysis. Consequently, the CO_2 electrolysers are anticipated to undergo a super-fast charging phase to generate formate for energy storage, whereas the microbial electrochemical reactor can facilitate a long-duration discharging phase by consuming formate for energy recovery. The configuration and operation of CO_2 electrolysers were optimized. For example, to underscore the significance of the slim-catholyte layer (Figure S1), additional CO_2 electrolysers as documented in previous studies were also developed (Figure S2).[10–11] In addition, two stand-by models of CO_2 electrolysers were compared. Furthermore, the electric signal generated from microbial electrochemical reactor was used for water biotoxicity monitoring. Moreover, the GDE and bioelectrode were systematically characterized to provide new insights of the mechanism study.

Results and Discussion

The CO_2 electrolyser with a slim-catholyte layer and a solid electrolyte layer was built. The cathode was Bi/C GDE, which was manufactured with commercially available Bi nanoparticles and carbon black. Parameters, such as catholyte KOH concentration and cell voltage, were optimized. Results of linear sweep voltammetry (LSV, Figure 1a) and electrochemical impedance spectroscopy (EIS, Figure 1b)

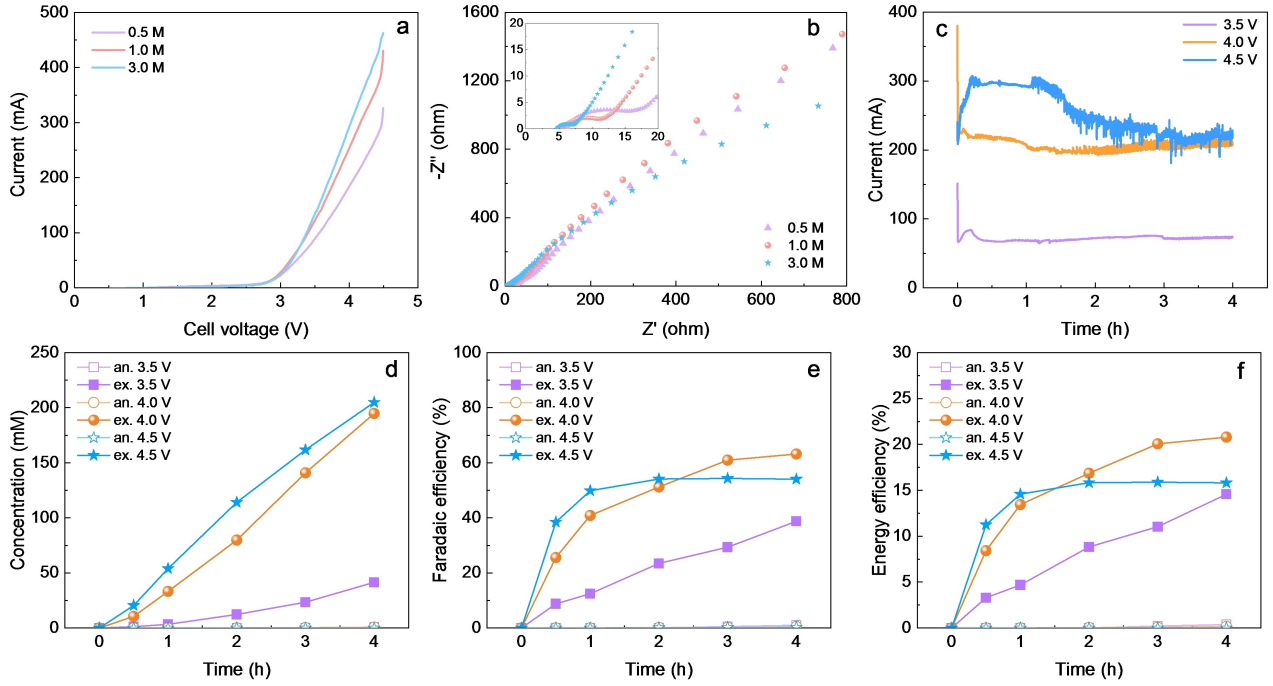

Figure 1. Optimization of CO_2 electrolysers. (a) LSV and (b) EIS curves at different catholyte KOH concentration. The insert displayed a zoomed-in view of the high frequency region. (c) Current, (d) formate concentration, (e) Faradaic efficiency, and (f) Energy efficiency at various cell voltages and a KOH concentration of 1.0 M. Abbreviation: an., anode; ex., extraction.

demonstrated that an increased catholyte KOH concentration enhanced the performance of the CO_2 electrolysers by reducing its internal resistance. For example, at 4.0 V, the current of the CO_2 electrolysers reached 294 mA (3.0 M KOH), 255.2 mA (1.0 M KOH), and 185 mA (0.5 M KOH), respectively. Please take note that when using 0.5 M and 1.0 M KOH, the current exhibited a rapid increase at a cell voltage of approximately 4.5 V. On the contrary, when using 3.0 M KOH, the increase trend of the current is consistent with the initial trend. When conducting LSV in a three-electrode system, a consistent trend of current increase is typically observed, irrespective of any variations in KOH concentration.[16] However, it's worth noting that a rapid increase in current has been reported upon reaching a specific cell voltage when LSV is carried out using a two-electrode configuration.[17] Therefore, the increase in cell voltage may not result in an equivalent shift in the cathode potential, and their difference could be influenced to some extent by the KOH concentration. However, it is important to mention that this intriguing phenomenon is not anticipated to have a significant impact on CO_2RR, considering that the majority of membrane electrode assembly (MEA)-based CO_2 electrolysers were operated at a cell voltage below 4.5 V.[7b] The EIS curves showed that the ohmic resistance was decreased from 6.2 Ω (0.5 M KOH) to 5.6 Ω (1.0 M KOH), and then further decreased to 4.7 Ω (3.0 M KOH). In addition, the catholyte KOH concentration influenced the activation resistance, as evidenced by a shift in the diameter of the first semicircle. In CO_2 electrolysers, the presence of high alkaline conditions is expected to facilitate high current density while suppressing the hydrogen evolution reaction.[18] Several promotion effects of alkali cations have been proposed for CO_2RR, including modifying the local electric field, buffering interfacial pH, altering water structure, and influencing reaction intermediates.[19] Furthermore, the presence of free ions can initiate the electrochemical reaction on the inner surface by facilitating ion conduction.[20] However, the using of extremely high catholyte KOH concentration might restrict the stability of CO_2 electrolysers, which is prone to the formation of carbonate salts.[21] Thus, the commonly used catholyte, 1.0 M KOH, was evaluated in the rest sections.

There was an observable trend of increasing current as the cell voltage increased (Figure 1c). However, there were some interesting observations in the data. At a voltage of 4.5 V, the current initially showed significant fluctuations in the first hour. Afterward, it decreased from around 300 mA to a value similar to that observed at 4.0 V, stabilizing at approximately 210 mA. Conversely, when operating at a constant voltage of 3.5 V, the current remained stable but at a lower level, approximately 70 mA. The initial fluctuation in current observed at 4.5 V was believed to be caused by a decrease in pH of the KOH solution, resulting from the reaction between hydroxide ions (OH^-) and CO_2.[22] This reaction could subsequently lead to an increase in the solution's resistance.[23] It's worth noting that when operated at 4.5 V and 4.0 V, respectively, the current eventually stabilized at a similar level (Figure 1c). Moreover, the final pH of the catholyte (Figure S3) also remained consistently close. The decrease in pH of the extraction solution was attributed to the buildup of un-ionized formic acid.[10–11] Additionally, the limited volume of catholyte (10 mL) exacerbated the decline in its pH.[21] To ensure a high current generation during CO_2RR in alkaline media, a commonly used approach is the periodic refreshing of the catholyte.[24] However, it is important to note that in the context of this study, this method may lead to a slight decrease in formate recovery within the extraction chamber.

Generally, the cell voltage plays a crucial role in determining the formate concentration and the recovery of electrons and energy in different chambers. Formate produced by CO_2RR was primarily recovered in the extraction chamber, with concentrations reaching approximately 200 mM at both 4.5 V and 4.0 V (Figure 1d). At a voltage of 4.0 V, the total Faradaic efficiency reached its highest point of 81.4 %, among which 63.2 % was obtained in the extraction solution, 17.7 % in the catholyte, and 0.5 % in the anolyte (Figure 1e, Figure S3, and Table S1). The full-cell rather than half-cell Energy efficiency of CO_2 electrolysers was calculated. Accordingly, the maximum total Energy efficiency was 26.8 % at 4.0 V, among which 20.8 % was recovered in the extraction solution, 5.8 % in the catholyte, and 0.2 % in the anolyte (Figure 1f, Figure S3, and Table S2).

When the Bi/C GDE was directly covered with Sustainion X37-50 anion exchange membrane (AEM), the current of the CO_2 electrolyser stabilized at 80 mA (Figure S4). This value closely matches the current observed in previous studies, even when advanced catalysts were utilized.[17] However, when the low-cost AEM (TWEDA1, approximately $80 per square meter from local company) was used, current of only 12 mA was observed.

Please note that Sustainion is widely adopted by many groups for CO_2RR due to its low area specific resistance, water mass balance, and robust stability.[7b] However, the practical implementation of Sustainion in scaling up electrolysers faces challenges such as liquid product crossover, fragility, and high cost (approximately $6000 per square meter from a foreign trade corporation). In summary, the incorporation of a slim-catholyte layer and solid electrolyte layer has enabled the utilization of affordable AEM and readily available catalysts for the direct and highly efficient production of pure formic acid from CO_2RR.

Stability evaluation of CO_2 electrolysers was conducted at 4.0 V (Figure S5). In the single-pass mode, the formate concentration reached its peak of 218 mM at the 2nd hour and remained above 150 mM for the first 10 hours. A similar trend was observed for Faradaic efficiency, with values exceeding 73 % during the initial 10 hours. Throughout the entire 30-hour reaction, a significant portion of electrons and energy were successfully recovered in the extraction solution, resulting in a Faradaic efficiency of 55.3 % and an Energy efficiency of 18.2 %. In contrast, the contribution of formate dissolved in the catholyte and anolyte was less than 1 %.

The stability of CO_2RR presents a systematic challenge, which can be attributed to three main factors:[25] (a) an increase in resistance as the pH value of the KOH solution

decreases;[23] (b) changes in the microenvironment due to flooding and salt accumulation, leading to blockage of mass transfer channels;[25–26] and (c) direct degradation of the electrocatalyst.[27] It is worth noting that the majority of studies on CO_2RR have reported stability tests spanned only a couple of hours.[7a] Additionally, it has been observed that direct exposure of the GDE to a KOH solution could stimulate salt accumulation, compared to a neutral electrolyte.[28]

The purity of the formate solution produced from the CO_2 electrolyser was verified. It was found that the potassium content in the formate solution could accumulate as high as 35.8 mg L^{-1} within just 4 hours when the extraction solution was circulated (Table S3). However, when the extraction solution was flowed in a single-pass mode during a 30-hour operation, the concentration of potassium was only 3.8 mg L^{-1} (Table S4). Other ions, such as copper, iron, sodium, bismuth, and silver, were generally found to be below 0.2 mg L^{-1}. These impurity ions have been previously reported, and their concentrations in the extraction solution can vary significantly, ranging from 10 ppb to 100 ppm, depending on the operational parameters.[10,29] Please note that the potassium and sodium contents were significantly reduced when the Sustainion X37-50 AEM directly covered the Bi/C GDE (Table S5). However, it is important to note that even with their maximum values in this study, potassium and sodium have high biocompatibility and are not expected to cause apoptosis.[11b]

The Gas Stand-By model, which involved storing N_2 gas in the extraction chamber during stand-by periods, was implemented for the first time, resulting in a total duration of 164 hours. The actual working time, during which a voltage of 4.0 V was applied, was calculated to be 12.6 hours. Unfortunately, performance degradation was still observed as the number of cycles increased. The current decreased from over 250 mA in the first cycle to 156 mA in the fifth cycle, and further decreased to 91 mA in the ninth cycle (Figure 2a). As a result, the concentration of formate in the effluent of the extraction solution decreased from 202 mM in the first cycle to 65 mM in the ninth cycle (Figure 2b). However, the maximum Faradaic efficiency of 80.2 % was observed in the fourth cycle, and throughout the entire operation, a value above 55.3 % was consistently maintained.

During the charging phase, the formate solution collected from the extraction chamber of CO_2 electrolysers was directly used to fuel the microbial electrochemical reactor (Figure 2c). This innovative biohybrid battery enabled super-fast charging and long-duration discharging. For example, the microbial electrochemical reactors were efficiently charged within a mere 3 minutes using the CO_2 electrolyzers, while a considerably longer discharging phase of 25 hours was observed. Theoretically, a single CO_2 electrolyser, with a working time of 12.6 hours, can be used to charge 252 microbial electrochemical reactors, each for 3 minutes.

It is worth noting that the recorded cell voltage in the microbial electrochemical reactors (below 150 mV) was significantly lower than the peaks observed during the 48-day acclimation process, which reached nearly 350 mV (Figure S6). A theoretical maximum cell voltage (1.23 V) can be calculated by considering the theoretical standard electrode potential at pH 7.0 when coupling HCO_3^-/formate (−0.41 V versus SHE) with H_2O/O_2 (+0.82 V versus

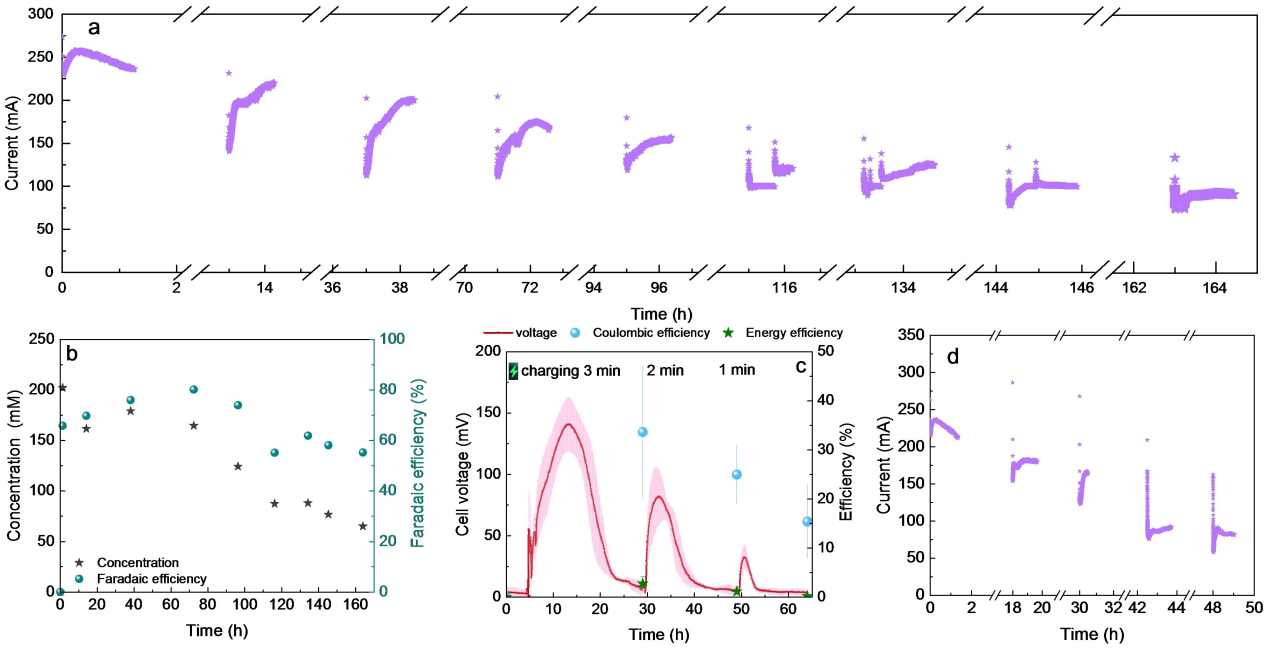

Figure 2. Charging and discharging of the biohybrid battery. (a) Current generation, and (b) formate concentration and Faradaic efficiency of CO_2 electrolysers when Gas Stand-By model was applied. (c) Cell voltage, Coulombic efficiency, and Energy efficiency of microbial electrochemical reactors. (d) Current generation of CO_2 electrolysers when Water Stand-By model was applied.

SHE).[30] However, it is important to consider that factors such as anode overpotential, cathode overpotential, and ohmic drops can contribute to a decrease in the observed cell voltage.[31] For instance, a significant anode overpotential was expected, as the initial formate concentration after charging (ranging from 1.6 mM to 10 mM, Figure S7) was significantly lower than that of acclimation process (50 mM, Figure S6). It is worth mentioning that increasing the cell voltage of microbial electrochemical reactors can be easily achieved by improving the charging time or adjusting the flow rate of the extraction solution to increase the initial formate concentration. However, it is important to note that achieving a high cell voltage is not always necessary to fulfill the function of microbial electrochemical reactors. For instance, in water biotoxicity monitoring, the main objective is to track changes in the electric signal under toxic stress.[15] Therefore, achieving a high cell voltage or power density in microbial electrochemical sensors may not necessarily be the ultimate goal in this context.

In the microbial electrochemical reactors, after a charging period of 3 minutes, a Coulombic efficiency of 33.6 ± 13.4 % and an Energy efficiency of 2.8 ± 1.4 % were observed. When taking into account the total Faradaic efficiency of 81.4 % and total Energy efficiency of 26.8 % from the CO_2 electrolysers, the overall Faradaic efficiency (27.4 %) and Energy efficiency (0.8 %) of the power-to-formate-to-bioelectricity process were calculated. The efficiencies achieved in this study for both microbial electrochemistry and CO_2 electrolysis were remarkably impressive, approaching the highest reported levels when compared to previous studies. In terms of formate production from CO_2 electrolysis, Faradaic efficiencies ranging from 40 % to nearly 100 % have been observed.[7c] Furthermore, full-cell Energy efficiencies ranging from 19 % to 31 % have been reported.[7c] The limited full-cell Energy efficiency is primarily attributed to the anodic oxygen evolution reaction (OER), which can consume up to 90 % of the electrical energy in CO_2RR.[32] It is worth noting that in formate-fed microbial electrochemical reactors, both the Coulombic efficiency and Energy efficiency are generally lower compared to reactors fed with the more commonly used acetate. For example, when using enriched communities to generate electric energy from formate, the Coulombic efficiency was measured at 5.3 %.[33] However, when a recombinant strain of *Escherichia coli* was employed for formate degradation, the Coulombic efficiency showed a significant increase, reaching 21.7 %.[34] In acetate-fed microbial electrochemical reactors that utilize separator material and U-shaped current collectors, the estimated Energy efficiency ranges from 21 % to 35 %.[35] However, in the case of a formate-fed reactor, the Energy efficiency was found to be as low as 0.151 %.[14a] These findings emphasize the significant impact of bioconversion in limiting both the overall Faradaic efficiency and Energy efficiency.

When applying the Water Stand-By model to CO_2 electrolyzers by storing water in the extraction chamber during stand-by periods (Figure 2d), a significant decline in current was observed, with only 81 mA recorded in the 5th cycle. Moreover, the current could not be restored even when the catholyte was refreshed. These findings indicate that, aside from issues such as the pH decrease of the KOH solution, the degradation of the GDE may be the main factor contributing to the instability of CO_2 electrolyzers.[18–19]

It is important to note that this novel biohybrid battery was characterized by a long discharging time, making it suitable for water biotoxicity monitoring. Once the cell voltage reached a stable state, a specific volume of methanal solution (Figure 3a) and Cu^{2+} solution (Figure 3b) was added to the microbial electrochemical reactors, respectively. During exposure to toxicants, it was observed that the normalized electrical signal (NES) decreased, and the reactors exposed to higher levels of toxicants showed more pronounced changes. For instance, after 30 minutes, the inhibition ratios were determined to be 9.3 % (0.1 % methanal) and 17.3 % (5.0 mg L^{-1} Cu^{2+}), respectively. Importantly, after refreshing the medium and charging with the CO_2 electrolysers, the microbial electrochemical reactors showed almost full recovery (Figure 3c). It is worth noting that the observed toxic response in this study aligns with previous reports on microbial electrochemical sensors.[15] Furthermore, there are various engineering strategies available to further enhance their performance, such as cell configuration design, sensing element choice, shear stress

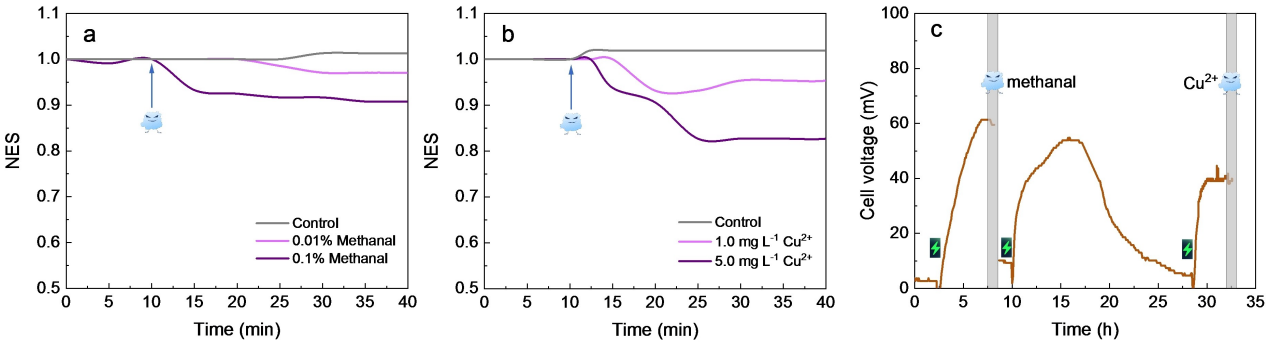

Figure 3. Water biotoxicity monitoring using the electric signal of microbial electrochemical reactors. (a) NES after methanal shock. (b) NES after Cu^{2+} shock. (c) The cell voltage profile of a typical microbial electrochemical reactor, showcasing the various steps of charging, discharging, monitoring, and recovery.

control, and electrical indicator selection.[36] In contrast to most microbial electrochemical sensors, where the repeatability is often limited by the bioanode,[15] this study observed that the degradation of the Pt/C cathode reduced the repeatability (Figure S8). The degradation of the Pt/C cathode could be attributed to the growth of heterotrophic microbes, as well as the biotic/abiotic generation of poisoning intermediates from formate.[37]

Characterization of both pristine and used Bi/C GDEs was conducted. In the pristine Bi/C GDE, planes with the highest intensity were assigned to Bi (012), Bi (104), and Bi (110), indicating a high degree of crystallinity in the Bi nanostructures (Figure 4a). However, after 30 hours of CO_2RR, the intensities of Bi (003), Bi (012), Bi (104), Bi (110), and Bi (202) reduced in the used GDE. Furthermore, the intensities of Bi (015) and Bi (107) were completely absent. In contrast, the intensity of Bi (101) was strengthened, and a new peak attributed to Bi (021) emerged. It is worth noting that during CO_2RR, researchers frequently observe morphological reconstruction, which can result in the formation of defect-rich Bi catalysts, leading to improved formate production.[38] However, it is crucial to note that these coordinately unsaturated defect sites are susceptible to attack and poisoning by oxygenated species, which ultimately leads to the degradation of the Bi catalysts.[27]

Cross-sectional scanning electron microscopy-energy dispersive X-ray spectrometry (SEM-EDS) elemental mapping of the Bi/C GDE was conducted (Figure 4b, Figure 4c, and Figure S9). The weight percentage of potassium (K) increased from 0.01 % (pristine) to 3.2 % (used), while the percentage of bismuth (Bi) rose from 0.7 % (pristine) to 4.5 % (used). The observed outcomes may be attributed to flooding, which facilitated the migration of K and Bi elements across the GDE.[18] The contact angle of Bi/C GDE decreased from 144.5 to 87.1 (Figure S10), indicating an enhanced hydrophilicity during CO_2RR.[9,39]

Based on the cyclic voltammetry (CV) curves of Bi/C GDE (Figure S11), the double-layer capacitance (C_{dl}) of the pristine electrode was determined to be 4.29 mF cm^{-2}, whereas for the used electrode, it increased to 10.25 mF cm^{-2} (Figure 4d). It is worth noting that the C_{dl} value calculated in this study is several times higher than that reported in previous studies,[40] primarily due to the use of capacitive carbon black. Furthermore, the observed alteration in the capacitance characteristics after CO_2RR indicates the potential for catalyst transmutation, which aligns with the findings from the X-ray diffraction (XRD) spectra. The anode (Pt–Ti) used for OER demonstrated exceptional stability, showing minimal electrochemical, structural, and morphological changes following CO_2RR (Figure S12).

The microbial analysis revealed an intriguing response of community structure to toxic stress in the bioanode. In general, *Proteobacteria* exhibited a volcano-shaped dependence, *Actinobacteriota* showed a decline, and *Bacteroidota* demonstrated an increase when exposed to high levels of toxicants (Figure 4e). In the used air cathode, *Proteobacteria* (86.01 %) and *Bacteroidota* (11.2 %) were the dominant microbial species.

At the genus level (Figure 4f), the model EAB *Geobacter* (ranging from 2.9 % to 6.2 %) was identified in the bioanode, and its abundance displayed a volcano-shaped dependence on the levels of toxicants. Furthermore, other

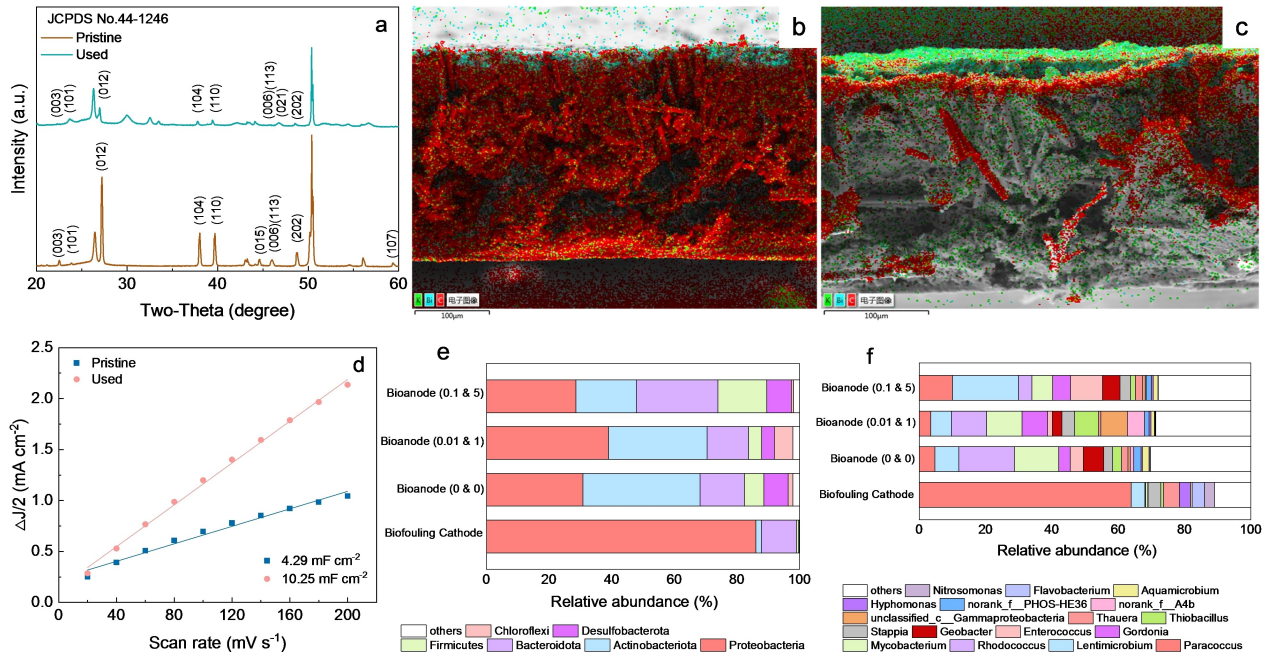

Figure 4. Characterization of the Bi/C GDE and bioelectrode. (a) XRD spectra of GDE. Cross-sectional SEM-EDS elemental mapping of (b) pristine and (c) used GDE. The color green represents the element K, blue represents Bi, and red represents C. (d) C_{dl} of GDE calculated based on CV curves. The relative abundance of microbes at the (e) phylum and (f) genus level. The numbers marked on the y-axis represent the concentrations of methanal (0, 0.01 %, and 0.1 %) and Cu^{2+} (0 mg L^{-1}, 1.0 mg L^{-1}, and 5.0 mg L^{-1}) that were exposed.

potential EAB genera,[41] including *Enterococcus* (ranging from 1.4 % to 9.6 %) and *Thiobacillus* (ranging from 1.5 % to 7.2 %) were also observed. The dominant microbe identified in the used air cathode was *Paracoccus* (63.9 %), which has also been found to be the prevailing bacteria in cathodic microbial communities in previous studies.[42] The functional analysis of the microbial community between the bioanodes with and without toxicants exposure was conducted utilizing the KEGG (Kyoto Encyclopedia of Genes and Genomes) database. Results revealed that toxicants exposure significantly impacted microbial functions related to the two-component system, carbon metabolism, and biosynthesis of secondary metabolites (Figure S13). Notably, the most prominent divergence was observed in the area of carbon metabolism, potentially attributable to the utilization of formate as the primary substrate by bioanodes. Formate can be utilized as a carbon and energy source by EAB, such as *Geobactor*.[14] The functional annotation suggested that FDH in the bioanodes could catalyze the first reaction in the Wood–Ljungdahl pathway (WLP). Additionally, formate-dissimilating and formate lyase pathways were suggested to potentially involved in pyruvate synthesis from formate.

In this study, the implementation of the power-to-formate-to-bioelectricity process allows biohybrid batteries to showcase a remarkable super-fast charging capability, enabling them to achieve high rates of CO_2 fixation and efficient energy storage. Furthermore, the extended discharging time of these batteries ensures their suitability for specific niche applications, such as water biotoxicity monitoring, as demonstrated. In future studies, it is recommended to systematically address issues discussed below.

Biohybrid batteries have the potential to serve as a flexible platform technology. Considering the remarkable advancements in the synthesis of formate from CO_2RR in recent decades,[43] it was selected as the energy carrier in this biohybrid battery. However, bioconversion of formate was proven to be a crucial factor in limiting overall efficiencies. The utilization of multi-carbon compounds, such as acetate, could offer a broader range of bioconversion options compared to formate.[44] However, the economic viability of generating multi-carbon compounds from CO_2RR is still a significant challenge.[45] As a result, in the absence of advanced electrocatalysts, the limitations of CO_2RR, rather than bioconversion, might hinder the overall efficiencies of the biohybrid battery when considering the use of acetate as an alternative to formate. The electricity recovered during the discharging phase has the potential to be utilized in various application scenarios that require a low power density but a long duration. Some examples include providing energy to wireless telemetry systems, powering the in situ microbial electrochemical treatment of nitrate-contaminated groundwater, and assisting in the desalination of low-concentration saltwater.[46] In this study, single-chamber air cathode microbial electrochemical reactors were constructed. This straightforward configuration enables the complete utilization of the substrate[31] and is particularly suitable for water biotoxicity monitoring.[15] However, it is important to note that this configuration may result in lower electron and energy recovery due to the crossover of oxygen and substrate between the anode and cathode.[31] Hence, in future studies, the configuration of microbial electrochemical reactors should be customized to suit specific applications.

Establishing evaluation metrics for the biohybrid battery is of utmost importance. This can be achieved by incorporating new metrics or refining the existing framework used for batteries assessment. Basic parameters such as current, voltage, and operating temperature can be easily obtained. For batteries study, it is crucial to report key metrics such as Coulombic efficiency, rate, capacity, and cyclability to provide a comprehensive and accurate assessment of performance.[47] Coulombic efficiency is defined as the ratio of discharge capacity to charge capacity in a single cycle of batteries. When considering the biohybrid battery, it is recommended to evaluate the overall Faradaic efficiency. This can be calculated by comparing the charge recovery from microbial electrochemical reactors to the charge storage in CO_2 electrolyzers within one cycle. The charge/discharge rate, commonly referred to as C-rate, is determined by the theoretical specific capacity of the electrode active material and the quantity present in batteries. In the case of the biohybrid battery, the capacity can be determined by considering the concentration of energy carriers and the volume of electrolyte within the microbial electrochemical reactors. The areal capacity of microbial electrochemical reactors was calculated to be 3.83 $mAh\,cm^{-2}$ for 50 mM of formate and 10 mL of electrolyte, which is comparable to the energy-dense lithium-ion batteries.[48] Galvanostatic charge/discharge is a commonly used method to evaluate the specific capacity and cyclability of batteries. However, in the case of the biohybrid battery, this method may not be applicable due to three main factors. Firstly, conducting automated experiments using battery test systems becomes challenging with the biohybrid battery due to the requirement for different anodes and cathodes in the charge/discharge processes. Secondly, unlike conventional batteries where the charge and discharge currents are typically set at the same value using a fixed C-rate, this practice is not recommended for the biohybrid battery, which is known for their super-fast charging and long-duration discharging capabilities. Thirdly, galvanostatic discharge is rarely used to assess microbial electrochemical reactors, except for evaluating the abiotic capacitance of electrodes or bio-capacitance of enriched microbes.[49] This method is not suitable for measuring the Faradaic reaction of energy carriers due to its invasive nature, which has the potential to cause cellular damage. Hence, it is not recommended to utilize the rate performance and cycling performance as evaluation metrics for the biohybrid battery.

The performance of the biohybrid battery can be enhanced even further. The rate and cell potentials of the CO_2 electrolyzer can be easily controlled using a battery test system. Ensuring the stability of CO_2RR poses a systematic challenge, but it can be improved through proper operation.[25] For instance, pulsed electrocatalysis has emerged as a novel in situ method to enhance the stability of CO_2 electrolyzers by reducing the formation of carbonate salts,[50] or by modulating the oxidation state of

electrocatalysts.[51] Therefore, to improve the operational stability of the biohybrid battery, which involves alternating "on" and "off" operating regimes, parameters like duty cycle and frequency can be further adjusted. Microbial electrochemical reactors have been reported to operate continuously for over a year,[52] and this study also showed stable power generation for 48 days (Figure S6). The discharge of microbial electrochemical reactors can be achieved either by using a fixed external resistor, as demonstrated in this study, or by employing the potentiostatic mode with the inclusion of a reference electrode.[31] Enhancing the tolerance of microbes to high concentrations of energy carriers can increase the capacity of the biohybrid battery. Furthermore, improving the tolerance of microbes to starvation can also reduce the cut-off values of cell voltage or current.

Conclusion

This study presented an innovative biohybrid battery that combines microbial electrochemistry with CO_2 electrolysis. The CO_2 electrolyzers were constructed with a slim-catholyte layer and a solid electrolyte layer, allowing for the use of a cost-effective AEM and a commercially available catalyst to produce pure formic acid as the energy carrier. Remarkably, the biohybrid battery demonstrated the capability to sustain a 25-hour discharging phase following a mere 3-minute charging period. Thanks to the Gas Stand-By model, the CO_2 electrolyzers operated continuously for a total duration of 164 hours. During the discharging phase, successful monitoring of water biotoxicity was accomplished. The systematic characterization of the GDE and bioelectrode provided valuable insights into the mechanisms and strategies for enhancing performance. To advance this flexible platform technology, future research should prioritize establishing comprehensive evaluation metrics and customizing it to meet specific application needs.

Acknowledgements

This work was supported by the National Natural Science Foundation of China (52370033, 31970106) and CAS Key Laboratory of Environmental and Applied Microbiology & Environmental Microbiology Key Laboratory of Sichuan Province, Chengdu Institute of Biology, Chinese Academy of Sciences (KLCAS-2023-1).

Conflict of Interest

The authors declare no conflict of interest.

Data Availability Statement

The data that support the findings of this study are available from the corresponding author upon reasonable request.

Keywords: Biosensor · Carbon Dioxide Reduction · Gas Diffusion Electrodes · Microbial Electrochemical Technology · Renewable Energy Storage

[1] Q. Y. Lin, X. Zhang, T. Wang, C. H. Zheng, X. Gao, *Engineering* **2022**, *14*, 27–32.
[2] a) F. M. Schwarz, J. Moon, F. Oswald, V. Müller, *Joule* **2022**, *6*, 1304–1319; b) J. Ma, L. Li, H. Wang, Y. Du, J. Ma, X. Zhang, Z. Wang, *Engineering* **2022**, *14*, 33–43.
[3] a) Q. Wang, S. Kalathil, C. Pornrungroj, C. D. Sahm, E. Reisner, *Nat. Catal.* **2022**, *5*, 633–641; b) N. Chu, W. Hao, Q. Wu, Q. Liang, Y. Jiang, P. Liang, Z. Jason Ren, R. Jianxiong Zeng, *Engineering* **2022**, *16*, 141–153.
[4] H. S. Shafaat, J. Y. Yang, *Nat. Catal.* **2021**, *4*, 928–933.
[5] H. M. Dietrich, R. D. Righetto, A. Kumar, W. Wietrzynski, R. Trischler, S. K. Schuller, J. Wagner, F. M. Schwarz, B. D. Engel, V. Müller, J. M. Schuller, *Nature* **2022**, *607*, 823–830.
[6] a) J. C. Wood, J. Grové, E. Marcellin, J. K. Heffernan, S. Hu, Z. Yuan, B. Virdis, *Water Res.* **2021**, *201*, 117306; b) Y. Jiang, H. D. May, L. Lu, P. Liang, X. Huang, Z. J. Ren, *Water Res.* **2019**, *149*, 42–55.
[7] a) N. Chu, Y. Jiang, Q. Liang, P. Liu, D. Wang, X. Chen, D. Li, P. Liang, R. J. Zeng, Y. Zhang, *Environ. Sci. Technol.* **2023**, *57*, 4379–4395; b) Z. Zhang, X. Huang, Z. Chen, J. Zhu, B. Endrodi, C. Janaky, D. Deng, *Angew. Chem. Int. Ed.* **2023**, *62*, e202302789; c) K. Fernández-Caso, G. Díaz-Sainz, M. Alvarez-Guerra, A. Irabien, *ACS Energy Lett.* **2023**, *8*, 1992–2024.
[8] E. C. Hann, S. Overa, M. Harland-Dunaway, A. F. Narvaez, D. N. Le, M. L. Orozco-Cárdenas, F. Jiao, R. E. Jinkerson, *Nat. Food* **2022**, *3*, 461–471.
[9] R. I. Masel, Z. Liu, H. Yang, J. J. Kaczur, D. Carrillo, S. Ren, D. Salvatore, C. P. Berlinguette, *Nat. Nanotechnol.* **2021**, *16*, 118–128.
[10] C. Xia, P. Zhu, Q. Jiang, Y. Pan, W. Liang, E. Stavitski, H. N. Alshareef, H. Wang, *Nat. Energy* **2019**, *4*, 776–785.
[11] a) P. Zhu, H. Wang, *Nat. Catal.* **2021**, *4*, 943–951; b) T. Zheng, M. Zhang, L. Wu, S. Guo, X. Liu, J. Zhao, W. Xue, J. Li, C. Liu, X. Li, Q. Jiang, J. Bao, J. Zeng, T. Yu, C. Xia, *Nat. Catal.* **2022**, *5*, 388–396.
[12] H. Xiang, H. A. Miller, M. Bellini, H. Christensen, K. Scott, S. Rasul, E. H. Yu, *Sustain. Energy Fuels* **2020**, *4*, 277–284.
[13] K. P. Sokol, W. E. Robinson, A. R. Oliveira, S. Zacarias, C.-Y. Lee, C. Madden, A. Bassegoda, J. Hirst, I. A. C. Pereira, E. Reisner, *J. Am. Chem. Soc.* **2019**, *141*, 17498–17502.
[14] a) J. Kan, L. Hsu, A. C. M. Cheung, M. Pirbazari, K. H. Nealson, *Environ. Sci. Technol.* **2011**, *45*, 1139–1146; b) T. Zhang, X. C. Shi, R. Ding, K. Xu, P. L. Tremblay, *ISME J.* **2020**, *14*, 2078–2089.
[15] N. Chu, Q. Liang, W. Hao, Y. Jiang, P. Liang, R. J. Zeng, *Chem. Eng. J.* **2021**, *404*, 127053.
[16] C.-T. Dinh, T. Burdyny, M. G. Kibria, A. Seifitokaldani, C. M. Gabardo, F. P. García de Arquer, A. Kiani, J. P. Edwards, P. De Luna, O. S. Bushuyev, C. Zou, R. Quintero-Bermudez, Y. Pang, D. Sinton, E. H. Sargent, *Science* **2018**, *360*, 783–787.
[17] Z. Wang, Y. Zhou, D. Liu, R. Qi, C. Xia, M. Li, B. You, B. Y. Xia, *Angew. Chem. Int. Ed.* **2022**, *61*, e202200552.
[18] B. Endrodi, A. Samu, E. Kecsenovity, T. Halmagyi, D. Sebok, C. Janaky, *Nat. Energy* **2021**, *6*, 439–448.
[19] a) J. Y. Zhao, Y. Liu, W. Li, C. F. Wen, H. Q. Fu, H. Y. Yuan, P. F. Liu, H. G. Yang, *Chem Catal.* **2023**, *3*, 100471; b) X. Y. Li, T. Wang, Y. C. Cai, Z. D. Meng, J. W. Nan, J. Y. Ye, J. Yi, D. P. Zhan, N. Tian, Z. Y. Zhou, S. G. Sun, *Angew. Chem. Int. Ed.* **2023**, *62*, e202218669.
[20] W. Li, Z. Yin, Z. Gao, G. Wang, Z. Li, F. Wei, X. Wei, H. Peng, X. Hu, L. Xiao, J. Lu, L. Zhuang, *Nat. Energy* **2022**, *7*, 835–843.

[21] L. Ge, H. Rabiee, M. Li, S. Subramanian, Y. Zheng, J. H. Lee, T. Burdyny, H. Wang, *Chem* **2022**, *8*, 663–692.
[22] J. Gu, S. Liu, W. Ni, W. Ren, S. Haussener, X. Hu, *Nat. Catal.* **2022**, *5*, 268–276.
[23] M. Zhang, W. Wei, S. Zhou, D.-D. Ma, A. Cao, X.-T. Wu, Q.-L. Zhu, *Energy Environ. Sci.* **2021**, *14*, 4998–5008.
[24] G.-Y. Duan, X.-Q. Li, G.-R. Ding, L.-J. Han, B.-H. Xu, S.-J. Zhang, *Angew. Chem. Int. Ed.* **2022**, *61*, e202110657.
[25] W. Lai, Y. Qiao, Y. Wang, H. Huang, *Adv. Mater.* **2023**, *n/a*, 2306288.
[26] C.-T. Dinh, T. Burdyny, M. G. Kibria, A. Seifitokaldani, C. M. Gabardo, F. P. García de Arquer, A. Kiani, J. P. Edwards, P. De Luna, O. S. Bushuyev, *Science* **2018**, *360*, 783–787.
[27] J. Zhu, J. Li, R. Lu, R. Yu, S. Zhao, C. Li, L. Lv, L. Xia, X. Chen, W. Cai, J. Meng, W. Zhang, X. Pan, X. Hong, Y. Dai, Y. Mao, J. Li, L. Zhou, G. He, Q. Pang, Y. Zhao, C. Xia, Z. Wang, L. Dai, L. Mai, *Nat. Commun.* **2023**, *14*, 4670.
[28] P. Zhang, K. Chen, B. Xu, J. Li, C. Hu, J. S. Yuan, S. Y. Dai, *Chem* **2022**, *8*, 3363–3381.
[29] L. Fan, C. Xia, P. Zhu, Y. Lu, H. Wang, *Nat. Commun.* **2020**, *11*, 3633.
[30] K. Rabaey, R. A. Rozendal, *Nat. Rev. Microbiol.* **2010**, *8*, 706–716.
[31] B. E. Logan, B. Hamelers, R. Rozendal, U. Schröder, J. Keller, S. Freguia, P. Aelterman, W. Verstraete, K. Rabaey, *Environ. Sci. Technol.* **2006**, *40*, 5181–5192.
[32] Q. Chen, X. Wang, Y. Zhou, Y. Tan, H. Li, J. Fu, M. Liu, *Adv. Mater.* **2023**, *n/a*, 2303902.
[33] P. T. Ha, B. Tae, I. S. Chang, *Energy Fuels* **2008**, *22*, 164–168.
[34] Y. Ojima, T. Kawata, N. Matsuo, Y. Nishinoue, M. Taya, *Bioprocess Biosyst. Eng.* **2014**, *37*, 2005–2008.
[35] Y. Fan, S.-K. Han, H. Liu, *Energy Environ. Sci.* **2012**, *5*, 8273–8280.
[36] J. Zhai, S. Dong, *Curr. Opin. Electrochem.* **2022**, *34*, 100975.
[37] A. Cuesta, G. Cabello, C. Gutiérrez, M. Osawa, *Phys. Chem. Chem. Phys.* **2011**, *13*, 20091–20095.
[38] D. Yao, C. Tang, A. Vasileff, X. Zhi, Y. Jiao, S.-Z. Qiao, *Angew. Chem. Int. Ed.* **2021**, *60*, 18178–18184.
[39] C. Chen, X. Yan, Y. Wu, S. Liu, X. Zhang, X. Sun, Q. Zhu, H. Wu, B. Han, *Angew. Chem. Int. Ed.* **2022**, *61*, e202202607.
[40] M. Zhang, Z. Zhang, Z. Zhao, H. Huang, D. H. Anjum, D. Wang, J.-h. He, K.-W. Huang, *ACS Catal.* **2021**, *11*, 11103–11108.
[41] D. R. Lovley, D. E. Holmes, *Nat. Rev. Microbiol.* **2022**, *20*, 5–19.
[42] K. Rabaey, K. Van de Sompel, L. Maignien, N. Boon, P. Aelterman, P. Clauwaert, L. De Schamphelaire, H. T. Pham, J. Vermeulen, M. Verhaege, P. Lens, W. Verstraete, *Environ. Sci. Technol.* **2006**, *40*, 5218–5224.
[43] D. Wakerley, S. Lamaison, J. Wicks, A. Clemens, J. Feaster, D. Corral, S. A. Jaffer, A. Sarkar, M. Fontecave, E. B. Duoss, S. Baker, E. H. Sargent, T. F. Jaramillo, C. Hahn, *Nat. Energy* **2022**, *7*, 130–143.
[44] B. Molitor, A. Mishra, L. T. Angenent, *Energy Environ. Sci.* **2019**, *12*, 3515–3521.
[45] X. F. Qiu, J. R. Huang, C. Yu, Z. H. Zhao, H. L. Zhu, Z. Ke, P. Q. Liao, X. M. Chen, *Angew. Chem. Int. Ed.* **2022**, *61*, e202206470.
[46] a) A. Shantaram, H. Beyenal, R. Raajan, A. Veluchamy, Z. Lewandowski, *Environ. Sci. Technol.* **2005**, *39*, 5037–5042; b) Y. Yoon, B. Kim, M. Cho, *Water Res.* **2023**, *244*, 120482.
[47] A. Noori, M. F. El-Kady, M. S. Rahmanifar, R. B. Kaner, M. F. Mousavi, *Chem. Soc. Rev.* **2019**, *48*, 1272–1341.
[48] C.-Y. Wang, T. Liu, X.-G. Yang, S. Ge, N. V. Stanley, E. S. Rountree, Y. Leng, B. D. McCarthy, *Nature* **2022**, *611*, 485–490.
[49] F. Soavi, C. Santoro, *Curr. Opin. Electrochem.* **2020**, *22*, 1–8.
[50] Y. Xu, J. P. Edwards, S. Liu, R. K. Miao, J. E. Huang, C. M. Gabardo, C. P. O'Brien, J. Li, E. H. Sargent, D. Sinton, *ACS Energy Lett.* **2021**, *6*, 809–815.
[51] X. D. Zhang, T. Liu, C. Liu, D. S. Zheng, J. M. Huang, Q. W. Liu, W. W. Yuan, Y. Yin, L. R. Huang, M. Xu, Y. Li, Z. Y. Gu, *J. Am. Chem. Soc.* **2023**, *145*, 2195–2206.
[52] P. Liang, R. Duan, Y. Jiang, X. Zhang, Y. Qiu, X. Huang, *Water Res.* **2018**, *141*, 1–8.

Manuscript received: August 21, 2023
Accepted manuscript online: October 6, 2023
Version of record online: October 19, 2023